



ELSEVIER

Discrete Applied Mathematics 88 (1998) 83–102

DISCRETE  
APPLIED  
MATHEMATICS

## On the definition and the construction of pockets in macromolecules<sup>☆</sup>

Herbert Edelsbrunner<sup>a,\*</sup>, Michael Facello<sup>b</sup>, Jie Liang<sup>c</sup>

<sup>a</sup> *Department of Computer Science, University of Illinois at Urbana-Champaign, USA*

<sup>b</sup> *Department of Computer Science and National Center for Supercomputing Applications,  
University of Illinois at Urbana-Champaign, USA*

<sup>c</sup> *Biophysics Division of the School of Life Sciences, National Center for Supercomputing Applications,  
and Department of Computer Science, University of Illinois at Urbana-Champaign, USA*

Received 20 March 1997; received in revised form 10 October 1997; accepted 15 April 1998

---

### Abstract

The shape of a protein is important for its functions. This includes the location and size of identifiable regions in its complement space. We formally define pockets as regions in the complement with limited accessibility from the outside. Pockets can be efficiently constructed by an algorithm based on alpha complexes. The algorithm is implemented and applied to proteins with known three-dimensional conformations. 1998 Published by Elsevier Science B.V. All rights reserved.

*Keywords:* Combinatorial geometry and topology; Algorithms; Molecular biology; Molecular modeling; Docking; Space filling and solvent accessible models; Voronoi cells; Delaunay simplices; Alpha complexes

---

### 1. Introduction

The motivation for the work reported in this paper is the apparent difficulty to talk in mathematically concrete terms about intuitive geometric concepts sometimes referred to as ‘depressions’, ‘canyons’, ‘cavities’, and the like. In topology, the notions of homotopy and homology have long been used to define and study (perfect) holes of various types and dimensions. We are after a definition and study of *imperfect* holes, of regions people would instinctively refer to as holes although they are neither holes in the homotopical nor the homological sense.

---

<sup>☆</sup> This work is partially supported by the Office of Naval Research, grant N00014-95-1-0691, and by the National Science Foundation through the Alan T. Waterman award, grant CCR-9118874, and the CISE postdoctoral fellowship, NSF grant ASC-9404900.

\* Corresponding author. E-mail: edels@cs.uiuc.edu.

Observations about common language reveal a great deal of confusion (or hidden wisdom?) on what holes are. A hole in the ground is usually a depression deep or big enough so we would care about its existence. The fact we can fall into but not through it reveals it is not a hole in a topological sense. Or consider exploding a balloon by poking through its surface with a needle. The needle connects the hole holding the balloon's air with the outside. Topologically, poking a needle through the surface removes rather than creates a hole.

*Pockets in proteins.* The study of imperfect holes in this paper focuses on proteins and other macromolecules. The ideas are more general though and can be extended to other 3-dimensional shapes and to higher dimensions.

The functions of a protein are determined through its interaction with other molecules. Such interactions happen frequently in protected yet accessible regions of appropriate size and shape. The shape complimentary between such a protected binding site and the ligand is largely responsible for the specificity observed in protein–ligand/protein interactions. There are also the less frequent situations where the binding ligand sits in an isolated cavity/void and is completely engulfed by the protein (such as the Xe binding sites in myoglobin). For such cases, we refer to our earlier results in cavity/void identification and their area and volume measurements [10]. The above intuitive but vague description of protein binding pockets is certainly not sufficient to distinguish protected regions from unprotected ones, or to specify the precise location and extent of a protected region once it is identified. In this paper, we will formally define pockets as regions in the complement space with limited accessibility from the outside. The definition deliberately excludes shallow valleys or depressions. Although there are also binding sites of the latter type, their determination will either require a priori knowledge or an extension of the ideas described in this paper.

*Intuition.* The following intuition guides our formulation of an unambiguous criterion. We declare a region in the complement a pocket if it can be reached only via relatively narrow pathways: “all paths into the pocket get narrow before they get wider”. This intuition can also be captured through a continuous growth process that simultaneously thickens every part of the protein: “a pocket becomes a void inaccessible from the outside before it disappears”.

It is clear that considerations based on relative distance are required to make this intuition concrete and algorithmically useful. Such considerations are expressed in terms of Voronoi cells [24] and Delaunay simplices [6]. These are key concepts in this paper and they play a crucial role in defining, delimiting, and algorithmically constructing pockets. The algorithm is implemented and sample applications to proteins whose coordinates are available from the protein databank are given.

*Outline.* Section 2 discusses common sphere models of molecules and their relationship to Voronoi cells. Section 3 describes dual sets and complexes of simplices. Section 4 defines pockets based on an acyclic relation over the Delaunay tetrahedra.

Section 5 presents an algorithm constructing pockets. Section 6 reviews problems on proteins where pocket computations have led to new insights. Section 7 mentions possible extensions of this work and directions for further research.

## 2. Spherical ball models

It is common in biology to represent an atom by a spherical ball and a molecule by a union of balls. Geometric models of this type go back to Lee and Richards [15] and Richards [20]. For a fixed set of atom centers, the *space filling* model uses van der Waals radii, see e.g. [5, Chapter 4], to unambiguously specify the balls and thus their union. The *solvent accessible* model increases radii to reflect accessibility for a solvent, itself modeled as a spherical ball. This section introduces the geometric terminology necessary to talk about these models and their relationship to Voronoi cells.

*Distance and growth.* The Euclidean distance between points  $x, y \in \mathbb{R}^3$  is denoted by  $|x - y|$ , and the (*spherical*) ball with center  $z \in \mathbb{R}^3$  and radius  $r \in \mathbb{R}$  is

$$b(z, r) = \{x \in \mathbb{R}^3 \mid |x - z| \leq r\}.$$

The union of a finite set  $B$  of balls is  $\bigcup B = \{x \in \mathbb{R}^3 \mid x \in b \in B\}$ . The complement,  $\mathbb{R}^3 - \bigcup B$ , consists of one or more components. Exactly one component is unbounded and usually referred to as the *outside*. The other components are bounded and referred to as *voids* of  $\bigcup B$ . Fig. 1 shows the union of a set of 2-dimensional balls or circular disks.

The solvent accessible model differs from the space filling model by the size of the balls; the centers are the same. This suggests we consider the union while growing the balls continuously and simultaneously. As the balls grow the union grows and the voids shrink. Which voids appear depends on the relative growth. We find it convenient to grow the balls such that the circles where two spheres meet sweep out a plane.

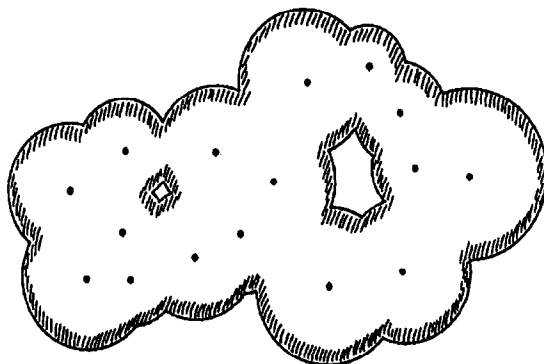


Fig. 1. The union of 16 disks is connected and decomposes its complement into 1 unbounded component (the outside) and 2 bounded components (voids).

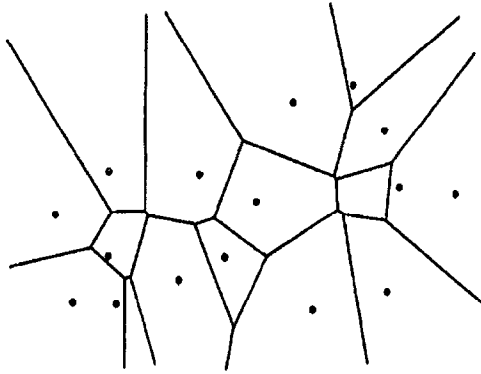


Fig. 2. The 16 disks in Fig. 1 define a decomposition of  $\mathbb{R}^2$  into 16 Voronoi cells.

The growth is controlled by a real parameter  $\alpha^2$ . Formally, we choose  $\alpha$  from  $\mathbb{R}^{1/2}$ , that is,  $\alpha$  is either a non-negative real or it is a positive real multiple of the imaginary unit,  $\sqrt{-1}$ . Define  $b_\alpha(z, r) = b(z, \sqrt{r^2 + \alpha^2})$  and

$$B_\alpha = \{b_\alpha(z, r) \mid b(z, r) \in B\}.$$

If  $r^2 + \alpha^2 < 0$ , the radius is imaginary and  $b_\alpha = b_\alpha(z, r)$  is empty. In this case,  $b_\alpha$  does not contribute to  $\bigcup B_\alpha$  but it does influence the formation of pockets. This makes sense since we argue pockets are regions that will *become* voids in the future. Future is defined in the direction of increasing  $\alpha^2$ , and  $b_\alpha$  is born when  $\alpha^2$  passes  $-r^2$ .

*Voronoi cells.* Define the *distance* of a point  $x \in \mathbb{R}^3$  from a ball  $b = b(z, r)$  as  $\pi_b(x) = |z - x|^2 - r^2$  and note it is defined even if  $r^2 < 0$ . In general,  $x \in b$  iff  $\pi_b(x) \leq 0$ . The *Voronoi cell* of  $b \in B$  is

$$V_b = \{x \in \mathbb{R}^3 \mid \pi_b(x) \leq \pi_c(x), c \in B\}.$$

In words,  $V_b$  is the set of points  $x$  at least as close to  $b$  as to any other ball in  $B$ . Define  $\text{Vor } B = \{V_b \mid b \in B\}$ . The set of points with equal distance from two balls form a plane. It follows  $V_b$  is the intersection of finitely many closed half-spaces and hence a convex polyhedron. Voronoi cells overlap at most along their boundary, and together they cover the entire space:  $\mathbb{R}^3 = \bigcup \text{Vor } B$ , see Fig. 2. The vertices, edges, and facets of the Voronoi cells are referred to as *Voronoi vertices*, *Voronoi edges*, and *Voronoi facets*. It is convenient to assume general position so every Voronoi edge belongs to exactly 3 Voronoi cells and every Voronoi vertex belongs to exactly 4 Voronoi cells.

Observe a point  $x \in \mathbb{R}^3$  is simultaneously contained in a ball  $c \in B$  and the Voronoi cell  $V_b$  of  $b \neq c$  only if  $\pi_b(x) \leq \pi_c(x) \leq 0$ . This implies  $x \in b$ . In other words,  $V_b \cap \bigcup B = V_b \cap b$  for every  $b \in B$ . The sets  $R_b = V_b \cap b$  are convex and any two overlap at most along their boundary. Define  $\text{Res } B = \{R_b \mid b \in B\}$  and note it covers the union of balls:  $\bigcup B = \bigcup \text{Res } B$ , see Fig. 4.

The growth process is defined so Voronoi cells do not change. Indeed,  $\pi_b(x) \leq \pi_c(x)$  iff  $\pi_{b_x}(x) \leq \pi_{c_x}(x)$ , and therefore  $\text{Vor } B = \text{Vor } B_x$  for every  $x \in \mathbb{R}^{1/2}$ . This will be important later when we take advantage of the fact the same Voronoi cells decompose every  $\bigcup B_x$  into convex cells.

### 3. Simplex collections

The connectivity of a union of balls can be expressed by a collection of simplices that keeps track of which cells  $R_b$  overlap. This collection is used to represent the union. Similarly, sets of simplices are used to represent voids and later pockets. We begin by introducing some general terminology.

*Simplicial complexes.* An abstract simplicial complex is a finite system of sets,  $\mathcal{A}$ , with  $X \in \mathcal{A}$  and  $Y \subseteq X$  implying  $Y \in \mathcal{A}$ .  $X \in \mathcal{A}$  is referred to as an abstract simplex and its dimension is  $\dim X = \text{card } X - 1$ . The vertex set is  $\text{Vert } \mathcal{A} = \bigcup \mathcal{A}$ . A subcomplex is an abstract simplicial complex  $\mathcal{B} \subseteq \mathcal{A}$ . For example, if  $S$  is any finite set, then the nerve of  $S$ ,

$$\text{Nrv } S = \left\{ X \subseteq S \mid \bigcap X \neq \emptyset \right\},$$

is an abstract simplicial complex with vertex set  $S$ . The nerve of every subset of  $S$  is a subcomplex of  $\text{Nrv } S$ . More generally, if  $S'$  is a collection of sets and  $i: S' \rightarrow S$  is an injection with  $a' \subseteq i(a')$  for each  $a' \in S'$  then  $\text{Nrv } S'$  is isomorphic to a subcomplex of  $\text{Nrv } S$ . Indeed,  $\mathcal{B} = \{X \subseteq S \mid X = i(X'), X' \in \text{Nrv } S'\}$  is clearly a subcomplex of  $\text{Nrv } S$  and isomorphic to  $\text{Nrv } S'$ .

Every abstract simplicial complex,  $\mathcal{A}$ , can be realized geometrically by a collection of simplices in  $\mathbb{R}^d$ , for some finite dimension  $d$ . The elements of  $\text{Vert } \mathcal{A}$  are represented by points, and an abstract simplex,  $X \in \mathcal{A}$ , is represented by the convex hull of the corresponding points. Provided  $d$  is large enough, the points can always be chosen so the convex hull is a simplex of dimension  $\dim X$  and no two simplices intersect improperly. Formally, let  $\iota: \text{Vert } \mathcal{A} \rightarrow \mathbb{R}^d$  be an injection so

$$\text{conv } \iota(X) \cap \text{conv } \iota(Y) = \text{conv } \iota(X \cap Y)$$

for all  $X, Y \in \mathcal{A}$ . The resulting set of simplices,

$$\mathcal{K} = \{ \text{conv } \iota(X) \mid X \in \mathcal{A} \},$$

is a (geometric) simplicial complex. The underlying space of  $\mathcal{K}$  is the union of simplex interiors:  $|\mathcal{K}| = \bigcup_{\sigma \in \mathcal{K}} \text{int } \sigma$ . In the case of a simplicial complex, the union of interiors is the same as the union of simplices. A subcomplex of  $\mathcal{K}$  is a set  $\{ \text{conv } \iota(X) \mid X \in \mathcal{B} \}$ ,  $\mathcal{B}$  a subcomplex of  $\mathcal{A}$ .

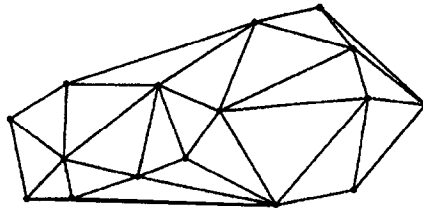


Fig. 3. The Delaunay complex of the 16 disks in Fig. 1.

*Delaunay simplices.* We form simplices by taking convex hulls of 1, 2, 3, or 4 ball centers. The collection of such simplices reflecting the overlap relation among the Voronoi cells is a complex which is now formally introduced.

Let  $B$  be a finite set of balls in  $\mathbb{R}^3$ , assume general position, and recall  $\text{Vor } B$  is the set of Voronoi cells. The nerve of  $\text{Vor } B$  is of course an abstract simplicial complex. It is geometrically realized by mapping each Voronoi cell to the center of the generating ball. Formally, let  $\iota: \text{Vor } B \rightarrow \mathbb{R}^3$  be defined by  $\iota(V_b) = z$  if  $b = b(z, r)$ . The *Delaunay complex* of  $B$  is

$$\text{Del } B = \{ \text{conv } \iota(X) \mid X \in \text{Nrv } \text{Vor } B \},$$

see Fig. 3. General position implies  $\text{Del } B$  is indeed a simplicial complex. The simplices  $\sigma \in \text{Del } B$  are referred to as *Delaunay simplices*.

Consider a tetrahedron  $\tau = \text{conv } \iota(X)$  in  $\text{Del } B$ . The 4 Voronoi cells in  $X$  intersect at a point  $z_\tau = \bigcap X$  referred to as the *orthogonal center* of  $\tau$ . Let  $b_1, b_2, b_3, b_4$  be the balls generating the Voronoi cells in  $X$ . By construction, the distance of  $z_\tau$  from the balls is the same:

$$r_\tau^2 = \pi_{b_1}(z_\tau) = \pi_{b_2}(z_\tau) = \pi_{b_3}(z_\tau) = \pi_{b_4}(z_\tau).$$

The *radius* of  $\tau$  is  $r_\tau$  and the *orthogonal ball* is  $b_\tau = (z_\tau, r_\tau)$ . The name suggests  $b_\tau$  meets the  $b_i$  in some ways orthogonally. Indeed, for a point on two intersecting spheres,  $x = \text{bd } b_\tau \cap \text{bd } b_i$ , the two tangent planes passing through  $x$  meet at a right angle.

*Alpha complexes.* The union of balls covers only a portion of the Voronoi cells, and this portion is represented by a subcomplex of the Delaunay complex, see [13].

Recall the definitions of  $R_b = V_b \cap b$  and  $\text{Res } B = \{R_b \mid b \in B\}$ . The nerve of  $\text{Res } B$  is an abstract simplicial complex that can be geometrically realized by mapping cells to ball centers, the same way as before. Let  $\iota: \text{Res } B \rightarrow \mathbb{R}^3$  be defined by  $\iota(R_b) = z$  with  $b = (z, r)$ . The *dual complex* of  $\bigcup B$  is

$$\text{Cpx } B = \{ \text{conv } \iota(X) \mid X \in \text{Nrv } \text{Res } B \},$$

see Fig. 4. Clearly,  $\text{Nrv } \text{Res } B$  is isomorphic to a subcomplex of  $\text{Nrv } \text{Vor } B$ , and therefore  $\text{Cpx } B \subseteq \text{Del } B$ . The dual complex inherits the property of being a simplicial complex from  $\text{Del } B$ .

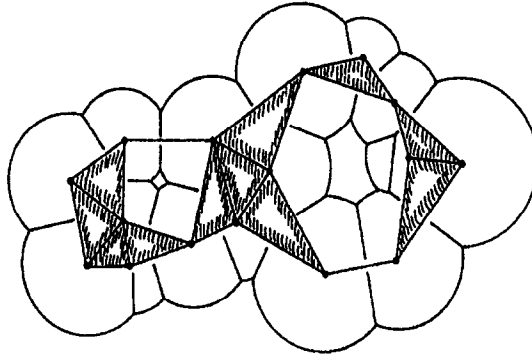


Fig. 4. The union of disks in Fig. 1 is decomposed into convex cells. The dual complex connects 2 centers by an edge and 3 centers by a triangle if the corresponding cells have non-empty common intersection. The union of disks has 2 voids, each contained in a void of the dual complex.

We refer to [8] for a list of properties  $CpxB$  enjoys. This includes  $CpxB$  is homotopy equivalent to  $\bigcup B$ . More precisely,  $|CpxB| \subseteq \bigcup B$  and there is a deformation retraction that takes  $\bigcup B$  to  $|CpxB|$ . The same is true for the respective complements. More precisely, each void of  $\bigcup B$  is contained in a void of  $|CpxB|$  and there is a deformation retraction that takes  $\mathbb{R}^3 - |CpxB|$  to  $\mathbb{R}^3 - \bigcup B$ .

Recall the definition of  $B_\alpha$ , which is obtained by simultaneously growing or shrinking all balls in  $B$ . The  $\alpha$ -complex of  $B$  is the dual complex of  $\bigcup B_\alpha$ :  $Cpx_\alpha B = Cpx B_\alpha$ . For  $\alpha_1^2 \leq \alpha_2^2$  we have  $B_{\alpha_1} \subseteq B_{\alpha_2}$ , which implies

$$\{\emptyset\} \subseteq Cpx_{\alpha_1} B \subseteq Cpx_{\alpha_2} B \subseteq Del B.$$

The bounds are tight. For sufficiently small  $\alpha^2$  all balls have imaginary radius and are empty, which implies  $Cpx_\alpha B = \{\emptyset\}$ . For sufficiently large  $\alpha^2$  the nerves of  $Res B$  and  $Vor B = Vor B_\alpha$  are isomorphic, which implies  $Cpx_\alpha B = Del B$ .

*The dual set of a void.* Recall a void of  $\bigcup B$  is a bounded component of the complement. To be specific, let

$$\mathbb{R}^3 - \bigcup B = H_0 \cup H_1 \cup \dots \cup H_k$$

be the partition into maximal connected subsets. Assume  $H_0$  is unbounded and  $H_1$  through  $H_k$  are the voids of  $\bigcup B$ . As mentioned earlier, there is a deformation retraction that takes the complement of  $|CpxB|$  to the complement of  $\bigcup B$ . Let

$$\mathbb{R}^3 - |CpxB| = H'_0 \cup H'_1 \cup \dots \cup H'_k$$

be the partition into components so the above mentioned deformation retraction takes  $H'_i$  to  $H_i$ , see Fig. 4. The voids of  $|CpxB|$  are naturally represented by the simplices in  $Del B - CpxB$  that cover them. For  $1 \leq i \leq k$  the *dual set* of  $H_i$  is

$$\mathcal{H}_i = \{\sigma \in Del B \mid \text{int } \sigma \subseteq H'_i\}.$$

For example, the smaller of the two voids in Fig. 4 has a dual set consisting of 2 triangles and 1 edge. The dual set of the larger void consists of 4 triangles and 3 edges. As shown in [8], the volume and surface area of a void  $H_i$  can be computed directly from  $\mathcal{H}_i$ , without explicit construction of  $H_i$ .

#### 4. Pockets

The concept of a pocket is based on an acyclic relation over the set of Delaunay tetrahedra motivated by a continuous flow field. After defining and classifying pockets we compare them with related concepts in the literature.

*Flow relation.* Let  $T'$  be the set of tetrahedra in  $\text{Del} B$  and  $T = T' \cup \{\tau_\infty\}$ , where  $\tau_\infty = \text{cl}(\mathbb{R}^3 - |\text{Del} B|)$  is a dummy element. We define the *flow relation* ' $\prec$ '  $\subseteq T \times T$  with  $\tau \prec \sigma$  if

- (i)  $\tau$  and  $\sigma$  share a common triangle,  $\varphi$ , and
  - (ii)  $\text{int } \tau$  and the orthogonal center  $z_\tau$  of  $\tau$  lie on different sides of the plane  $\text{aff } \varphi$ .
- The conditions makes sense for  $\sigma = \tau_\infty$  but not for  $\tau = \tau_\infty$ . The flow relation is acyclic because  $\tau \prec \sigma$  implies  $r_\tau^2 < r_\sigma^2$  or  $\sigma = \tau_\infty$ . In words, the radius of the orthogonal ball increases with the flow relation. This is the intuition behind the flow or vector field that motivates the definition of ' $\prec$ ': a point flows in the direction of the closest orthogonal ball whose radius exceeds the distance of the point from the closest ball in  $B$ .

If  $\tau \prec \sigma$  we call  $\tau$  a *predecessor* of  $\sigma$  and  $\sigma$  a *successor* of  $\tau$ . The set of *descendants* of  $\tau$  is

$$\text{Des } \tau = \{\tau\} \cup \bigcup_{\tau \prec \sigma \in T} \text{Des } \sigma,$$

and the set of *ancestors* of  $\sigma$  is

$$\text{Anc } \sigma = \{\sigma\} \cup \bigcup_{\sigma \succ \tau \in T} \text{Anc } \tau.$$

$\sigma \in T$  is a *sink* if it has no successors, or equivalently  $\text{Des } \sigma = \{\sigma\}$ .  $\tau_\infty$  is necessarily a sink. A tetrahedron  $\sigma \in T'$  is a sink iff it contains its orthogonal center:  $z_\sigma \in \sigma$ . In general,  $\sigma$  cannot have more than 3 successors because  $z_\sigma$  can be on the other side of at most 3 of the 4 triangles bounding  $\sigma$ .

Sinks are important since they are responsible for the formation of voids. Indeed, if  $H_i$  is a void of  $\bigcup B$  then at least one tetrahedron in  $\mathcal{H}_i$  is a sink. This follows from the observation that  $\tau \in \mathcal{H}_i$  and  $\tau \prec \sigma$  implies  $\sigma \in \mathcal{H}_i$ . If  $\sigma \in T$  is a sink that belongs to  $\mathcal{H}_i$  then  $z_\sigma \in H_i$  and  $r_\sigma^2 > 0$ . The radii of sinks thus predict the moment in time  $H_i$  will disappear, namely when  $\alpha$  reaches the maximum radius of any sink in  $\mathcal{H}_i$ . Of course, before  $H_i$  disappears it may break up into several voids, each with at least one sink.

*Pockets.* The point set topological notions of closure, interior, and boundary motivate analogous combinatorial notions applicable to sets of simplices. The *closure* of a subset



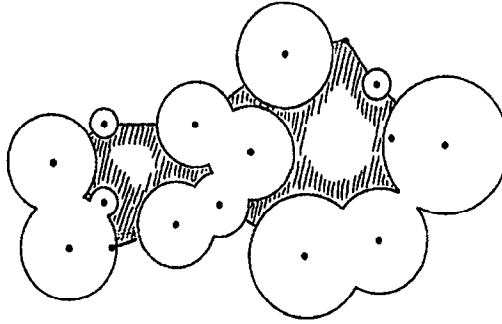


Fig. 5. The 16 disks are obtained by shrinking the disks in Fig. 1; 3 of them have now imaginary radii. There are 2 pockets each grown from one of the voids in Fig. 1. Consult Figs. 2 and 3 to see that 5 Delaunay triangles are ancestors of  $\tau_\infty$ . All other triangles belong to  $\mathcal{P}$  and none to the dual complex of the disk union. The component of 4 disks in the middle of the picture defines a chain of 4 vertices and 3 edges in the dual complex. This chain separates  $\mathcal{P}$  into 2 components, each defining a pocket.

$L$  of a simplicial complex  $\mathcal{X}$  is  $\text{Cl}L = \{\tau \in \mathcal{X} \mid \tau \subseteq \sigma \in L\}$ ; it is the smallest subcomplex that contains  $L$ . The *star* of  $\tau \in \mathcal{X}$  is  $\text{St} \tau = \{\sigma \in \mathcal{X} \mid \tau \subseteq \sigma\}$ .  $L \subseteq \mathcal{X}$  is *open* in  $\mathcal{X}$  if  $\text{St} \tau \subseteq L$  for every  $\tau \in L$ . The *interior* of a subset  $L \subseteq \mathcal{X}$  is  $\text{Int} L = \{\tau \in L \mid \text{St} \tau \subseteq L\}$ ; it is the largest open set contained in  $L$ . The *boundary* of  $L$  is  $\text{Bd} L = \text{Cl} L - \text{Int} L$ .  $L$  is *connected* if its underlying space is path-connected: for every two points  $x, y \in |L|$  there is a continuous path  $p : [0, 1] \rightarrow |L|$  with  $p(0) = x$  and  $p(1) = y$ . The *components* of  $L$  are the maximal connected subsets.

As mentioned earlier, the intention is to define pockets so they are generalizations of voids, possibly with connections to the outside. The relation over the tetrahedra decides which side tetrahedra belong and the divide forms the connection to the outside. More precisely, pockets consist of the Delaunay tetrahedra that do not belong to  $\text{Cpx} B$  and that are not ancestors of  $\tau_\infty$ . Define  $\mathcal{P} = \text{Cl}(T - \text{Anc} \tau_\infty) - \text{Cpx} B$ , and let

$$\mathcal{P} = \mathcal{P}_1 \dot{\cup} \mathcal{P}_2 \dot{\cup} \dots \dot{\cup} \mathcal{P}_k$$

be the partition into components. For each  $1 \leq i \leq k$ ,

$$P_i = \bigcup \mathcal{P}_i - \bigcup B$$

is a *pocket* of  $\bigcup B$ , and  $\mathcal{P}_i$  is its *dual set*. These definitions are illustrated in Fig. 5.

The above definition of pockets treats the unbounded component special and different from the voids. Sometimes this may not be appropriate and large voids are to be treated the same way as the unbounded component. This can formally be done by bounding the radii of the sinks used in the construction. For a size limit  $\beta^2 \in \mathbb{R}$  define  $T_\beta = \{\tau_\infty\} \cup \{\sigma \in T' \mid r_\sigma^2 > \beta^2\}$  and

$$\mathcal{P}_\beta = \text{Cl} \left( T - \bigcup_{\sigma \in T_\beta} \text{Anc} \sigma \right) - \text{Cpx} B.$$

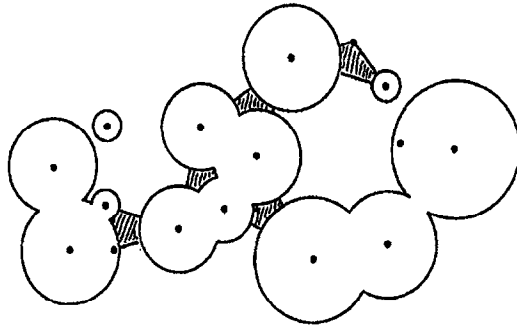


Fig. 6. The upper bound on the sink radii used for the example shown excludes sinks whose orthogonal centers are not covered by the disk union in Fig. 1. As a result, the 2 pockets in Fig. 5 are reduced to 5 smaller pockets.

As before, the subset of  $\mathbb{R}^3 - \bigcup B$  covered by the interiors of the simplices in a component of  $\mathcal{P}_\beta$  is a pocket, and the component is its dual set, see Fig. 6.

*Mouth openings.* The only type of pockets without connection to the outside are the voids. All other pockets connect to the outside at one or more places. For a pocket  $P_i$  consider the part of  $\text{Bd } \mathcal{P}_i$  not contained in  $\text{Cpx}B$ .  $\text{Bd } \mathcal{P}_i$  is a simplicial complex and connectedness and components relative to  $\text{Bd } \mathcal{P}_i$  are well defined for all its open subsets. The mentioned set is indeed open in  $\text{Bd } \mathcal{P}_i$  and we let

$$\text{Bd } \mathcal{P}_i - \text{Cpx}B = \mathcal{M}_1 \dot{\cup} \mathcal{M}_2 \dot{\cup} \dots \dot{\cup} \mathcal{M}_\ell$$

be the partition into components. The *mouths* of  $P_i$  are the sets  $M_j = \bigcup \mathcal{M}_j - \bigcup B$ , for  $1 \leq j \leq \ell$ , and their *dual sets* are the  $\mathcal{M}_j$ . Consider for example the two pockets in Fig. 5. The left and smaller pocket has 3 mouths, each defined by a single Delaunay edge. The right and bigger pocket has 4 mouths, 3 defined by a single Delaunay edge each and 1 defined by a chain of 2 Delaunay edges and 1 Delaunay vertex.

The number of mouths,  $\ell$ , is a useful characteristic of a pocket and can be used to distinguish between different types. One would expect a pocket with different number of mouths in a protein implies different functionalities. We suggest the following terminology reflecting the resulting classification. Call a pocket a

<i>void</i>	if $\ell = 0$ ,
<i>normal pocket</i>	if $\ell = 1$ ,
<i>simple connector</i>	if $\ell = 2$ ,
<i>multiple connector</i>	if $\ell \geq 3$ .

In the presence of a size limit one can furthermore distinguish between connectors whose mouths connect to the same or to different components of the outside.

*Related concepts.* The computational biology literature contains at least 3 concepts defined as tools to study regions of limited accessibility. These are the ‘molecular

surface’, the ‘interstitial skeleton’, and the ‘molecular interface’. We briefly point out the similarities and differences between pockets and these concepts. The authors of this paper believe pockets are superior to all 3 concepts in terms of visual appearance, objective quantification, and wide applicability.

The molecular surface model defined by Richards [20] is a union of balls,  $\bigcup B$ , where gaps inaccessible to a sphere modeling a solvent are filled. Let  $MS \supseteq \bigcup B$  be the resulting object. The union of pockets is similar to albeit not the same as the difference,  $MS - \bigcup B$ , union all voids of  $MS$ . While pockets are defined in terms of relative distance, the criterion employed for defining molecular surface uses absolute distance, namely the radius of the solvent. Furthermore, the object obtained from  $MS$  is cluttered with tiny remains within the crevices and cusps of  $\bigcup B$ . Pockets do not share this visual distraction.

The interstitial skeleton defined by Connolly [3] consists of all Voronoi edges outside  $\bigcup B$  and within the convex hull of the balls. A problematic feature of this concept is the lack of any possibility to clip edges inside delta regions where a depression opens up slowly towards the outside. Another disadvantage is the mess of edges that possibly attracts the eye to large pockets, but they offer little in terms of objective quantification.

The molecular interface has recently been suggested by Varshney and coauthors [23] to study the region between interacting molecules. It assumes 2 or more different molecules and consists of the points outside all molecules at distance at most  $\varepsilon$  from at least 2 of the molecules.  $\varepsilon$  is a parameter that can be chosen and adjusted. A shortcoming of this definition is its lack of dependence on any local shape characteristic. Also, it cannot be used to study depressions in a single molecule. On the other hand, pockets are easily adjusted to study the interface: compute pockets for the union of the molecules and select only the ones that touch at least 2 different molecules.

## 5. Algorithm

We construct pockets by growing them from sinks. We assume a pointer based data structure for  $\text{Del} B$  and a linear list that distinguishes between Delaunay simplices inside and outside an alpha complex. Both data structures are part of the alpha shape software [11], which forms the basis of our implementation. The entire software is based on exact arithmetic and the simulation of general position by infinitesimal perturbation [12]. We begin by describing the two data structures in sufficient detail to provide the context for the construction of pockets.

*Simplex digraph.* We refer to the pointer based data structure for  $\text{Del} B$  as the *simplex digraph*. It supports access to neighboring simplices in constant time each. Data structures with this functionality are reasonably standard and different versions have been described in the literature, see e.g. [1, 7].

The simplices of  $\text{Del} B$  are the nodes of the digraph, and they are referenced through pointers. Each simplex has direct access to its location in the linear list or filter, see

below. In order to avoid a tedious discussion of the details of the simplex digraph, we stipulate functions `FACES` and `COFACES` that provide access to the neighborhood. Given a simplex  $\sigma \in \text{Del } B$  and a dimension  $k < \dim \sigma$ , `FACES` returns the  $k$ -dimensional faces:

$$\text{FACES}(\sigma, k) = \{\tau \in \text{Cl}\{\sigma\} \mid \dim \tau = k\}.$$

For  $k > \dim \sigma$ , `COFACES` returns the  $k$ -dimensional simplices that share  $\sigma$  as a face:

$$\text{COFACES}(\sigma, k) = \{\tau \in \text{St } \sigma \mid \dim \tau = k\}.$$

It is convenient to assume `COFACES`( $\sigma, 3$ ) includes  $\tau_\infty$  if  $\sigma$  lies on the boundary of  $|\text{Del } B|$ . We assume both functions take constant time per returned simplex. As an example consider the problem of computing the set  $N(\sigma)$  of tetrahedra adjacent to a given tetrahedron  $\sigma \in \text{Del } B$ .

```

N( $\sigma$ ) :=  $\emptyset$ ;
for all  $\varphi \in \text{FACES}(\sigma, 2)$  do
  for both  $\tau \in \text{COFACES}(\varphi, 3)$  do
    if  $\tau \neq \sigma$  then  $N(\sigma) := N(\sigma) \cup \{\tau\}$  endif
  endfor
endfor.

```

The first loop is over 4 triangles and the second over 2 tetrahedra each, so the total time for finding all adjacent tetrahedra is constant.

*Filter and filtration.* The Delaunay simplices are stored in the order they enter the alpha complex. We assume an array representation with constant time access via indices. Recall the  $\alpha_1$ -complex of  $B$  is a subcomplex of the  $\alpha_2$ -complex if  $\alpha_1^2 \leq \alpha_2^2$ . It follows that the sequence of real numbers  $\alpha^2$  defines a sequence of nested complexes. Two consecutive complexes differ by one or more Delaunay simplices, and the cardinality of  $\text{Del } B$  is an upper bound on the number of complexes in the sequence. We represent the sequence by a list of simplices sorted in the order they enter. We break ties by letting vertices precede edges precede triangles precede tetrahedra. Remaining ties are broken arbitrarily. The resulting sequence of simplices,

$$\emptyset = \sigma_0, \sigma_1, \sigma_2, \dots, \sigma_n,$$

is a *filter* of  $\text{Del } B$ . The array is a representation of the filter, with pointers linking simplices to their locations in the simplex digraph. Each prefix of the filter defines a simplicial complex,  $\mathcal{K}_i = \{\sigma_0, \sigma_1, \dots, \sigma_i\}$ . The resulting sequence of complexes,

$$\{\emptyset\} = \mathcal{K}_0, \mathcal{K}_1, \mathcal{K}_2, \dots, \mathcal{K}_n = \text{Del } B,$$

is a *filtration* of  $\text{Del } B$ . For each  $\alpha^2 \in \mathbb{R}$  there is an index  $i(\alpha)$  with  $\text{Cpx}_\alpha B = \mathcal{K}_{i(\alpha)}$ , but not necessarily vice versa.

Suppose we wish to construct the pockets of  $\bigcup B_\alpha$ , or rather their dual sets. The general idea is to traverse the latter part of the filter, from  $\sigma_{i+1}$  to  $\sigma_n$ . The algorithm is incremental, and after processing the simplices in  $\mathcal{K}_j$  the data structures

represent the pockets for the corresponding size limit. Each encountered tetrahedron either joins the outside, joins a set of delayed tetrahedra because it does not belong to the current set of pockets, or starts a new pocket and possibly merges some of the existing pockets into one. The delayed tetrahedra will be added at the appropriate time.

*Representing pockets.* The pockets are stored as sets of tetrahedra in an evolving system,  $\mathcal{Y}$ , represented by a *union-find* data structure. The sets in  $\mathcal{Y}$  are pairwise disjoint and the data structure supports the following operations:

- ADD( $u$ ): Add  $\{u\}$  as a new set to  $\mathcal{Y}$ .
- SET( $u$ ): Find set  $X \in \mathcal{Y}$  with  $u \in X$ .
- UNION( $X, Y$ ): Replace sets  $X$  and  $Y$  by  $X \cup Y$ .

A sequence of  $m$  operations takes time  $O(m\alpha(m))$ , where  $\alpha(m)$  is the extremely slowly growing inverse of Ackermann’s function, see e.g. [4, Chapter V]. For all practical purposes,  $\alpha(m)$  can be considered a small constant.

In our application, the elements in the system are tetrahedra.  $\mathcal{Y}$  is initialized to  $\{\{\tau_\infty\}\}$ . SET( $\tau_\infty$ ) represents the outside and is the only set in  $\mathcal{Y}$  that does not represent a pocket.

*Traversing the filter.* The index of a simplex specifies its position in the filter. If  $\sigma_j$  is a tetrahedron its *depth* is

$$\begin{aligned} \text{dp } \sigma_j &= \max\{k \mid \sigma_k \in \text{Des } \sigma_j\} \\ &= \max(\{j\} \cup \{\text{dp } \tau \mid \sigma_j \prec \tau\}). \end{aligned}$$

The depth determines the minimum size limit from which moment on the tetrahedron belongs to the set of pockets. The recursive specification of depth lends itself to computing all depth values in a single traversal of the filter.

```

for  $j := n$  downto 1 do
  dp  $\sigma_j := j$ ;
  for all  $\tau \in N(\sigma_j)$  do
    if  $\sigma_j \prec \tau$  then dp  $\sigma_j := \max\{\text{dp } \sigma_j, \text{dp } \tau\}$  endif
  endfor
endfor.

```

Pockets are constructed by following the evolution of the ball growth. Only tetrahedra  $\sigma_j$  with  $i(\alpha) < j \leq i(\beta)$  need to be considered, and such a  $\sigma_j$  belongs to  $\mathcal{P}_\beta$  iff  $\text{dp } \sigma_j \leq i(\beta)$ . When the traversal reaches  $\sigma_j$ , all tetrahedra with depth  $j$  are added to the union-find system representing the pockets. These tetrahedra are collected in an initially empty set  $Y_j$ . At the time  $Y_j$  is processed it may or may not contain  $\sigma_j$ .

```

for  $j := i(\alpha) + 1$  to  $i(\beta)$  do
   $k := \text{dp } \sigma_j$ ;  $Y_k := Y_k \cup \{\sigma_j\}$ ;
  for all  $\sigma \in Y_j$  do
    ADD( $\sigma$ );
    for all  $\tau \in N(\sigma)$  with  $\tau \in \bigcup \mathcal{T}$  do
      let  $\varphi$  be the triangle shared by  $\tau$  and  $\sigma$ ;
      if  $\varphi \notin \text{Cpx}_\alpha B$  then UNION(SET( $\sigma$ ), SET( $\tau$ )) endif
    endfor
  endfor
endfor.

```

Note the test whether or not the tetrahedron  $\tau$  belongs to any set in  $\mathcal{T}$  that occurs in the inner for-loop. For  $\tau = \sigma_k$  the test is equivalent to  $i(\alpha) < k$  and  $\text{dp } \tau < j$ .

*Dual sets of pockets and mouths.* The traversal constructs a pocket  $P$  as a set of tetrahedra. To compute the dual set,  $\mathcal{P}$ , we still need to take the closure of this set and remove simplices in the dual complex of  $\bigcup B$ . Similarly, to get the dual sets of the mouths, we need to take the boundary, remove simplices in the dual complex, and collect components. We first describe the process for pockets and then for mouths.

Let  $X \in \mathcal{T}$  be the collection of tetrahedra defining  $P$ . The closure  $\mathcal{C} = \text{Cl } X$  is obtained by collecting all faces, with a straightforward marking mechanism to avoid duplication:

```

 $\mathcal{C} := X \cup \{\emptyset\}$ ;
for all  $\tau \in X$  do
   $\mathcal{C} := \mathcal{C} \cup \text{FACES}(\tau, 2) \cup \text{FACES}(\tau, 1) \cup \text{FACES}(\tau, 0)$ 
endfor.

```

The dual set of  $P$  is finally obtained by removing all simplices from  $\mathcal{C}$  whose indices in the filter are less than  $i(\alpha) + 1$ . The dual sets of the mouths  $M_j$  are the components  $\mathcal{M}_j$  of  $\text{Bd } \mathcal{P} - \text{Cpx } B$ . To construct them, we first compute  $\mathcal{I} = \text{Int } \text{Cl } X$  but making use of the fact that a vertex or edge in  $\mathcal{C}$  belongs to  $\mathcal{I}$  iff all triangles in its star belong to  $\mathcal{I}$ :

```

 $\mathcal{I} := \mathcal{C} - \{\emptyset\}$ ;
for all triangles  $\varphi \in \mathcal{I}$  do
  for both  $\tau \in \text{COFACES}(\varphi, 3)$  do
    if  $\tau \notin X$  then  $\mathcal{I} := \mathcal{I} - \{\varphi\} - \text{FACES}(\varphi, 1) - \text{FACES}(\varphi, 0)$  endif
  endfor
endfor.

```

Every boundary simplex of  $\mathcal{P}$  belongs to  $\mathcal{B} = \text{Bd } \text{Cl } X = \mathcal{C} - \mathcal{I}$  or to  $\text{Cpx } B$  or to both. We can therefore work with  $\mathcal{B}$ , which can be constructed along with  $\mathcal{I}$  by the above algorithm.  $\mathcal{B}$  is a 2-dimensional connected manifold because  $\mathcal{I}$  is connected.



Fig. 7. The alpha shape of gramacidin A reflecting the topological structure of the molecule.

This means every edge belongs to exactly 2 triangles and the star of every vertex is an alternating cycle of edges and triangles. The  $\mathcal{M}_j$  are the components of  $\mathcal{B} - \text{Cpx}B$ . They are computed in a way analogous to the computation of the dual sets of pockets, only in one dimension lower. First, traverse the triangles  $\varphi \in \mathcal{B}$  and collect the ones outside  $\text{Cpx}B$  in a system represented by a union-find data structure. Whenever a triangle is added, check the 3 adjacent triangles and merge sets if they are already in the system. In the end, each set  $Y$  in the system contains the triangles of a mouth  $M_j$ . The dual set of  $M_j$  is  $\mathcal{M}_j = \text{Int Cl } Y - \text{C}_{\text{px}}B$ .

## 6. Protein examples

In this section we give examples of pockets in proteins and of protein studies that gained new insights with the help of pockets.

*Tunnel extraction for Gramacidin A.* Gramacidin A is a synthetic membrane channel and has been used as an antibiotic. It is composed of D and L amino acid residues in alternating order. Fig. 7 shows the alpha complex of the molecule for  $\alpha=0$  to the left and for some larger value of  $\alpha$  to the right. Fig. 8 shows that the tunnel of the potassium channel is extracted by the pocket construction of gramacidin A.

*Inhibitor binding site of HIV-1 protease.* HIV-1 protease is an essential viral protease for the generation of mature structural proteins and enzymes of HIV. The protease is the target of several new inhibitor drugs that are part of the cocktail recipe for AIDS patients. The binding site of the HIV-1 protease is computed for one structure (pdb name 1hos) after removal of the inhibitor. It is the largest pocket on the protein, and the dual set can be seen in Fig. 9 (left, tetrahedra in solid), whereas the alpha complex of the enzyme is represented by wireframe. To the right, the corresponding atoms in the dual set are drawn as space filling balls using RASMOL [21].

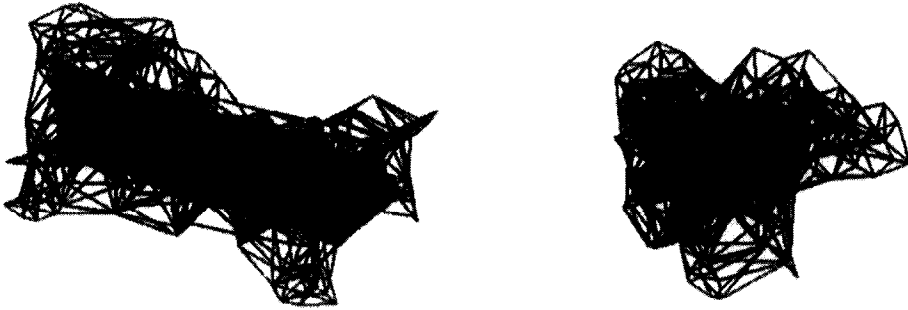


Fig. 8. The pocket constructed from the alpha shape model of gramacidin A shown in the right part of Fig. 7. It is a simple connector.

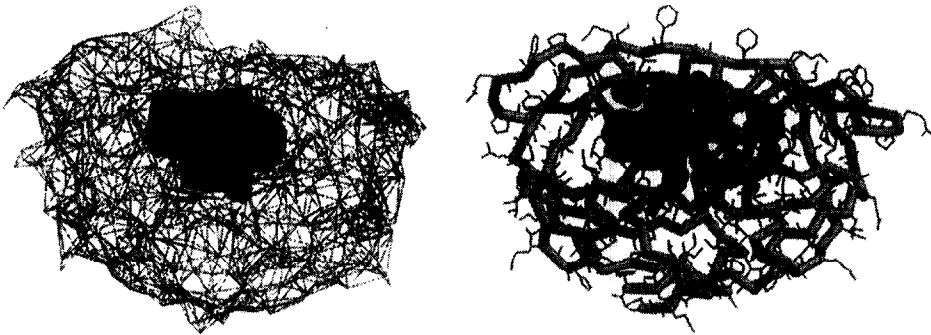


Fig. 9. The HIV-1 protease, (left) tetrahedra in the dual sets with gold mouth triangles, and (right) the dual set atoms shown in space filling balls, and the inhibitor in red.

*Binding site for FK506 immunosuppressant.* The protein that binds to the potent immunosuppressant FK506, the FK binding protein (FKBP), can block T cell activation and is involved in signal transduction of immune stimulation. The binding pocket (ivory) for FK506 in a X-ray structure (pdb name 1fkf) is shown in Fig. 10. The atoms in the dual set of the binding pocket for FK506 (red) are drawn in space filling balls. They are computed from the X-ray structure of FKBP after the removal of FK506. On the left hand side another pocket (green) can be seen in the vicinity.

A promising drug design strategy is the linked fragment method, where optimized compounds binding to different nearby pockets with moderate affinities can be linked to produce a high affinity ligand [18]. The two pockets of FKBP as shown in Fig. 10 indicate that FKBP is a good target protein amenable to such design strategy. Recently, a high affinity (9 nM) ligand for FKBP has been designed by linking two compounds of low affinities (2 and 100  $\mu$ M) [22]. NMR experiments have identified the residues that interact with the compounds, and all come from the two pockets shown in Fig. 10. Residues interacting only with the substrate-like compound, are in the ivory pocket,





Fig. 10. The active site of FK506 binding protein (ivory) and another pocket nearby (green).

residues interacting only with the second compound are in the green pocket, and those interacting with both are in the ivory pocket and are near the green pocket. Analysis based on pocket computation using the method described in this paper may therefore provide useful information about the selection of target protein a priori, the selection of compounds for pockets to avoid mutual steric exclusion, as well as the design of linker of the right length and geometry, see [16] for more details.

*Proton acceptor of redox-active tyrosine D in photosystem II.* Another application where pocket computation has provided important information is photosystem II (PSII). Almost all oxygen in the atmosphere is generated by the photosystem II in plant and algae. A redox-active tyrosine D in the D2 subunit of PS II plays important role. Tyrosine D releases its phenolic proton upon lighting. Identification of the acceptor of this proton is important for understanding the energetics of PSII.

Recently, mutants of His 189 of the D2 subunit have been generated and chemical rescue experiments have been conducted using imidazole to mimic histidine. Results suggest that His 189 is the proton acceptor. However, there is uncertainty about the existence of any empty space near His 189 to accommodate imidazole. Such structural support is now provided by the pocket analysis of analogous sites in bacterial reaction centers [14]. Fig. 11 shows the pocket containing both analogous residues to tyrosine D and His 189 on the structure of bacterial reaction center of *R. sphaeroides* (pdb name 4rcr). It has a volume of  $524 \text{ \AA}^3$ , large enough to allow imidazole (about  $86 \text{ \AA}^3$ ) to gain access. Similar pockets are found in all structures of bacterial reaction centers. This structural evidence of a pocket is further strengthened: compared to the full se-

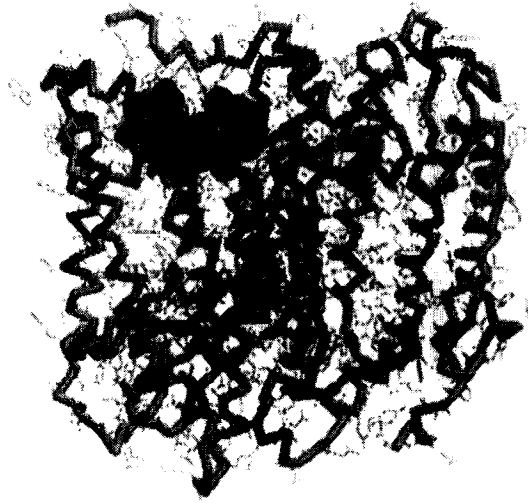


Fig. 11. The pocket near Arg 164 (red) and His 193 (yellow) of the M subunit of bacterial reaction center.

quences, the fragments that fold together forming this pocket have significantly higher sequence similarity across species among bacterial reaction centers and photosystem II.

*Analysis of protein hydration changes: correlation with experiments.* Water associated with the solvation of macromolecules play a fundamental role in biological processes. An experimental technique, called *osmotic stress* [2], probes protein hydration by observing the changes in biological process (equilibrium binding constants, reaction rates, etc.) with different concentrations of polymer in the system. These polymers in the bulk solution generate osmotic pressure, but are sterically too large to enter the protein hydration space. Changes in biological processes, when correlated with the changes in the osmotic stress, can be used to measure the number of hydration waters that are transferred during protein conformation changes. At the molecular level, the hydration spaces that exclude polymers are pockets on the protein surface and voids in the interior. Exactly polymer of what size is excluded is related to the mouth area of the pocket.

The pocket method has been applied to the analysis of the role of hydration in antithrombin III (aTIII), a protein involved in the blood clotting process and is of interest for cardiac disease. Fig. 12 shows the hydration space in the two conformations of aTIII, that is, the pockets and voids of size allowing at least two water molecules. As can be seen, the distribution and size of these pockets and voids are quite different for the two conformations of the same protein. The details and change in the volume of hydration space upon enzyme inhibition can be computed. In the study of aTIII, the calculated results are well in consistency with the release of about 70 water molecules to the bulk during I to L transformation, as measured by osmotic stress [17].



Fig. 12. The hydration space of the two conformations (I, left; L right) of antithrombin III that are large enough to contain two water molecules.

## 7. Discussion and extensions

Initial experiments have shown that the algorithm for computing pockets described in this paper cannot find shallow pockets. In systems of large molecules, shallow pockets can occur quite frequently. One possible solution to this problem is an additional parameter specifying ‘steepness’ or ‘speed’ of flow that will add finer control over the inclusion or exclusion of the tetrahedra that flow to  $\tau_\infty$ .

The concept of a pocket can be applied to the complementary space of a macromolecule thus defining protrusions of the molecule. An appropriate notion of complementarity is described in [9]. The authors of this paper expect that pockets and protrusion together provide a good handle on predicting docking pairs and sites.

The notion of limited accessibility arises also in studies of shapes in other fields. For example, Miller [19] uses it to compute realistic shadings of statues. Notions of local and global accessibility are related to molecular surfaces and to pockets. The algorithmic techniques in this paper can be used to improve the performance of the algorithms in [19] by orders of magnitudes.

## Acknowledgements

The authors thank Ping Fu and Ernst Mücke for their contributions to the alpha shapes software in which the pockets software is embedded.

## References

- [1] E. Brisson, Representing geometric structures in  $d$  dimensions: topology and order, *Discrete Comput. Geom.* 9 (1993) 387–426.

- [2] M.F. Colombo, D.C. Rau, V.A. Parsegian, Protein solvation in allosteric regulation: A water effect on hemoglobin, *Science* 256 (1992) 655–659.
- [3] T.H. Connolly, Molecular interstitial skeleton, *Comput. Chem.* 15 (1991) 37–45.
- [4] T.H. Cormen, Ch.E. Leiserson, R.L. Rivest, *Introduction to Algorithms*, MIT Press, Cambridge, MA, 1990.
- [5] T.E. Creighton, *Proteins. Structures and Molecular Principles*, Freeman, New York, 1984.
- [6] B. Delaunay, Sur la sphère vide, *Izv. Akad. Nauk SSSR, Otdelenie Matematicheskii i Estestvennyka Nauk* 7 (1934) 793–800.
- [7] D.P. Dobkin, M.J. Laszlo, Primitives for the manipulation of three-dimensional subdivisions, *Algorithmica* 4 (1989) 3–32.
- [8] H. Edelsbrunner, The union of balls and its dual shape, in: I. Bárány, J. Pach (Eds.), *László Fejes Tóth Festschrift, Discrete Comput. Geom.* 13 (1995), 415–440.
- [9] H. Edelsbrunner, Deformable smooth surface design, *Discrete Comput. Geom* (1998) to appear.
- [10] H. Edelsbrunner, M. Facello, P. Fu, J. Liang, Measuring proteins and voids in proteins, in: *Proc. 28th Hawaii Internat. Conf. Syst. Sci.*, 1995, pp. 256–264.
- [11] H. Edelsbrunner, M. Facello, P. Fu, E.P. Mücke (devs.), Three-dimensional alpha shapes, Software developed at the Univ. Illinois at Urbana-Champaign, Illinois, 1991–1996, <ftp.ncsa.uiuc.edu>.
- [12] H. Edelsbrunner, E.P. Mücke, Simulation of Simplicity: a technique to cope with degenerate cases in geometric algorithms, *ACM Trans. Graphics* 9 (1990) 66–104.
- [13] H. Edelsbrunner, E.P. Mücke, Three-dimensional alpha shapes, *ACM Trans. Graphics* 13 (1994) 43–72.
- [14] S. Kim, J. Liang, B.A. Barry, Chemical complementation identifies a proton acceptor for redox-active tyrosin D in photosystem II, *Proc. Natl. Acad. Sci. USA* 94 (1997) 14406–14411.
- [15] B. Lee, F.M. Richards, The interpretation of protein structures: estimation of static accessibility, *J. Mol. Biol.* 55 (1971) 379–400.
- [16] J. Liang, H. Edelsbrunner, C. Woodward, Anatomy of protein pockets and cavities: measurement of binding sites and implications for ligand design, *Protein Science*, in press.
- [17] J. Liang, M.P. McGee, Mechanisms of coagulation factor Xa inhibition by antithrombin: Correlation between hydration structures and water transfer during reactive loop insertion, *Biophys. J.* 75 (1998) 573–582.
- [18] C. Mattos, B. Rasmussen, X. Ding, G.A. Petsko, D. Ringe, Analogous inhibitors of elastase do not always bind analogously, *Struct. Biol.* 1 (1994) 55–58.
- [19] G. Miller, Efficient algorithms for local and global accessibility shading, *Comput. Graphics* 28 (1994) 319–326.
- [20] F.M. Richards, Areas, volumes, packing, and protein structures, *Ann. Rev. Biophys. Bioeng.* 6 (1977) 151–176.
- [21] R. Sayle, E.J. Milner-White, RasMol: biomolecular graphics for all, *Trends Biochem. Sci. TIBS-20* (1995) 374.
- [22] S.B. Shuker, P.J. Hajduk, R.P. Meadows, S.W. Fesik, Discovering high-affinity ligands for proteins: Sar by nmr, *Science* 274 (1996) 1531–1534.
- [23] A. Varshney, F.P. Brooks, Jr., D.C. Richardson, W.V. Wright, D. Manocha, Defining, computing, and visualizing molecular interfaces, in: *Proc. IEEE Visualization'95*, eds. G.M. Nielson and D. Silver (1995) pp. 36–43.
- [24] G. Voronoi, Nouvelles applications des paramètres continus à la théorie des formes quadratiques, *J. Reine Angew. Math.* 133 (1907) 97–178.